Published in final edited form as:
Transl Cancer Res. 2014 April 1; 3(2): 124–137. doi:10.3978/j.issn.2218-676X.2013.06.02.

Defining functional changes in the brain caused by targeted stereotaxic radiosurgery

Vipan K. Parihar, **Munjal M. Acharya**, **Dante E. Roa**, **Omar Bosch**, **Lori-Ann Christie**, and **Charles L. Limoli**
Department of Radiation Oncology, University of California Irvine, Irvine, CA 92697, USA

Abstract

Brain tumor patients routinely undergo cranial radiotherapy, and while beneficial, this treatment often results in debilitating cognitive dysfunction. This serious and unresolved problem has at present, no clinical recourse, and has driven our efforts to more clearly define the consequences of different brain irradiation paradigms on specific indices of cognitive performance and on the underlying cellular mechanisms believed to affect these processes. To accomplish this we have developed the capability to deliver highly focused X-ray beams to small and precisely defined volumes of the athymic rat brain, thereby providing more realistic simulations of clinical irradiation scenarios. Using this technique, termed stereotaxic radiosurgery, we evaluated the cognitive consequences of irradiation targeted to the hippocampus in one or both hemispheres of the brain, and compared that to whole brain irradiation. While whole brain irradiation was found to elicit significant deficits in novel place recognition and fear conditioning, standard platforms for quantifying hippocampal and non-hippocampal decrements, irradiation targeted to both hippocampi was only found to elicit deficits in fear conditioning. Cognitive decrements were more difficult to demonstrate in animals subjected to unilateral hippocampal ablation. Immunohistochemical staining for newly born immature (doublecortin positive) and mature (NeuN positive) neurons confirmed our capability to target irradiation to the neurogenic regions of the hippocampus. Stereotaxic radiosurgery (SRS) of the ipsilateral hemisphere reduced significantly the number of doublecortin and NeuN positive neurons by 80% and 27% respectively. Interestingly, neurogenesis on the contralateral side was upregulated in response to stereotaxic radiosurgery, where the number of doublecortin and NeuN positive neurons increased by 22% and 36% respectively. Neuroinflammation measured by immunostaining for activated microglia (ED1 positive cells) was significantly higher on the ipsilateral versus contralateral sides, as assessed throughout the various subfields of the hippocampus. These data suggest that certain cognitive decrements are linked to changes in neurogenesis, and that the unilaterally irradiated brain exhibits distinct neurogenic responses that may be regulated by regional differences in neuroinflammation. Compensatory upregulation of neurogenesis on the contralateral hemisphere may suffice to maintain cognition under certain dose limits. Our results demonstrate unique cognitive and neurogenic consequences as a result of targeted stereotaxic radiosurgery, and

Corresponding to: Prof. Charles L. Limoli. Department of Radiation Oncology, University of California Irvine, Medical Sciences I, Room B-146B, Irvine CA 92697-2695, USA. climoli@uci.edu.

Disclosure: The authors declare no conflict of interest.

suggest that these irradiation paradigms elicit responses distinct from those found after exposing the whole brain to more uniform radiation fields.

Keywords

Stereotaxic radiosurgery (SRS); radiation-induced cognitive dysfunction; neurogenesis; neuroinflammation

Introduction

Radiotherapy delivered as whole brain or partial brain irradiation remains a primary treatment modality for the control of primary and secondary brain malignancies (1). Recent advances in beam delivery have largely been developed to minimize unintended normal tissue toxicity, which limits the total dose that be safely administered. The fundamental goal of any treatment plan is to optimize the therapeutic ratio by minimizing dose to normal tissues while maximizing dose to the tumor. The evolution of contemporary modalities such as intensity modulated radiation therapy (IMRT) (2–4) and stereotaxic radiosurgery (SRS) (5,6) have thus improved normal tissue sparing to neurogenic and other critical brain regions and reduced late toxicities while increasing the total dose that can be applied to the tumor (7). While these advances have been beneficial, resultant cognitive deficits frequently occur and represent debilitating and persistent problems associated with cranial radiotherapy (8–12). Given the increased survival of patients diagnosed with brain cancer, quality of life in terms of cognitive health has become an increasing concern, especially in the absence of any satisfactory long-term treatments.

While the precise mechanisms of radiation-induced cognitive dysfunction remain largely unresolved, they are certain to be complex and multifaceted, involving tissues subjected to a range of doses that lie within and outside the treatment margins (1,13,14). While late effects involving white matter necrosis, demyelination and disruptions to the blood brain barrier occur at relatively higher doses (>40–50 Gy), cognitive decrements transpire at much lower doses and in the relative absence of any overt histomorphologic change (1,13,14). The response of the irradiated brain involves acute and protracted effects in which inflammatory and oxidative species can compromise the functionality and recovery of normal tissue. Significant evidence suggests that radiation-induced depletion of neural stem and progenitor cells plays a contributory if not causal role in the development of certain hippocampal learning and memory impairments (15–19). The subgranular zone (SGZ) of the hippocampal dentate gyrus (DG) is one site of active neurogenesis in which stem cells are born, proliferate, migrate and ultimately differentiate into granule cells neurons that can functionally integrate into the hippocampal circuitry (20). Microenvironmental changes in oxidative stress (21,22) and inflammation (23) coupled with the loss of hippocampal stem cells following irradiation act to inhibit neurogenesis and impair cognition. Precisely how these processes are affected by radiation treatments targeted to one or both hippocampi has not however been rigorously evaluated at doses that do not elicit significant late normal toxicity.

The capability to compare the consequences of high and low dose irradiation to specific regions of the brain would clearly facilitate an analysis of the mechanisms of brain injury that adversely impact cognition. Significant past work has evaluated the effects of whole brain irradiation (WBI) over relatively smaller doses (0.5–10 Gy) (16,24,25) or larger total doses delivered under various fractionation regimes (26–30). While these studies have contributed significantly to our current understanding of radiation effects in the brain, more systematic studies of cognition and neurogenesis under focal irradiation strategies have received less attention. Various options now exist for the focal delivery of irradiation, and several labs have utilized the gamma knife (GK) for targeting intracranial volumes with high accuracy (5,6). Many higher dose studies (>60 Gy) have compared responses from within and outside the target volume and found a range of gene expression changes that varied over time (31–36). However, at these high doses little unirradiated tissue remains, such that GK irradiation of rodents simulates clinical treatments combining lower dose WBI and higher dose SRS.

In the present work, we focused on a single dose of irradiation (10 Gy) known to cause cognitive deficits in the absence of other complicating normal tissue toxicity using our well-established athymic rat model (37,38). Ionizing radiation was delivered either as whole brain or as a highly focused beam to one or both hippocampi via linear accelerator (LINAC) based SRS. Irradiated animals were then subjected to cognitive testing 1 month afterwards, followed by an immunohistochemical assessment of radiation injury and neurogenic changes. Here we describe our findings showing distinct differences in cognitive and neurogenic responses between animals exposed to different irradiation paradigms.

Methods and materials

Animals

All animal procedures were carried out in accordance with NIH and Institutional Animal Care and Use Committee guidelines. Two-month old, male athymic nude (ATN) rats (strain 02N01 Cr: NIH-rnu) were obtained from National Cancer Institute and were maintained in the colony until they were 3 months of age. The ATN rat is a standard model used in xenograft studies that has proven to be a valuable tool in cancer research. Animals were group-housed in a specific pathogen-free room under controlled conditions (20±1 °C; 70% ±10% humidity). Artificial lighting was maintained on a 12:12 hour light:dark cycle, and animals had free access to a conventional diet and water. Experimental groups were as follows: N=4 bilateral hippocampal-only IRR (hIRR); N=6 unilateral hippocampal-only IRR (uhIRR); N=17 whole-brain IRR [N=9 for novel place recognition (NPR) testing and a separate cohort of N=8 for the fear conditioning (FC) testing, wbIRR]; N=20 sham-irradiated controls (N=12 for NPR testing and separate cohort of N=8 for FC testing, CON).

Treatment planning and stereotaxic radiosurgery (SRS)

Stereotactic radiosurgery (SRS) (39) in the form of intensity-modulated radiation therapy (IMRT) and volumetric-modulated arc therapy (VMAT) (40) were used to irradiate one hippocampus or both hippocampi, respectively. These treatment plans delivered total doses of 10 Gy to one or both hemispheres of the rat brain.

For the delivery of the SRS treatment, a representative ATN rat underwent treatment planning, in which MRI and CT scans comprising axial images of 0.8 mm thickness of the rat's skull were acquired. The MRI and CT images were transferred to Eclipse treatment planning software (Varian Medical Systems, Palo Alto, CA), where image fusion, target and organs-at-risk contouring, and modeling of the expected dose distribution inside the rodent's brain were performed. The structures contoured were the left and right hippocampi, whole brain, and brain excluding the hippocampus (Figure 1).

A 6-field non-coplanar IMRT plan was generated for irradiation of the left hippocampus while a co-planar two-arc VMAT plan irradiated both hippocampi (Figure 2). Dosimetric results calculated in Eclipse for the IMRT and VMAT plans showed that both plans provided conformal dose distributions to the targeted regions while minimizing dose to the remaining portion of the brain and to the contralateral hippocampus for the IMRT case. The 10 Gy, 8 Gy and 6 Gy isodose lines in the axial and sagittal views and around the hippocampal region are shown, while the dose volume histogram shows the dose sparing to the contralateral hippocampus that was achieved (Figure 3).

Treatment was delivered using a TG-51 (41) calibrated 6 MV photon beam produced by a radiotherapy Varian Trilogy LINAC equipped with an on-board imaging system (OBI). Prior to treatment, orthogonal diagnostic quality X-ray images (image dose <0.002 Gy) of the skull were taken with the OBI and were co-registered to digitally-reconstructed radiograph (DRR) images generated from the planning CT in Eclipse (Figure 4). Bony landmarks used in the co-registration provided information on positioning shifts required for precise setup of the rat on the treatment table prior to irradiation.

The SRS irradiations were performed with each rat under sedation for a period of approximately 45 minutes. An IMRT treatment which included setup and beam-on time lasted ~30 min while the VMAT treatment required ~10 min. After the treatment, the irradiated animal was transferred back to its cage in a quiet and warm area and allowed to recover.

Cognitive testing using the novel place recognition (NPR) and fear conditioning (FC) tasks 6 weeks following irradiation

Novel place recognition—In this task two open-field white acrylic arenas, each measuring 45 high, 70×70 cm^3 were used. Both the arenas were coupled with high-contrast extra maze spatial cues. A video camera was centered on the ceiling above each arena, and live tracking of the animals was achieved using Noldus Ethovision XT (version 7.0; Noldus Information Technology). Animals were habituated to the arena for 20 min daily for 2 days before commencement of the behavioral testing. The following day, in a familiarization phase of 3 minutes, rats were allowed to explore two identical blocks (8×3×10 cm^3 high) that were placed 27 cm from opposing corners of the arena. Rats were then returned to a holding cage for a 5-minute retention interval. Following this delay, an identical copy of one of these blocks was moved to an open corner at a distance of 18 cm from the arena wall ("novel place"), whereas an additional identical block remained at its former spatial location ("familiar place"). Rats were allowed to explore the stimuli freely for 3 minutes. For all phases, the "head direction to zone" function in Ethovision XT was used to track exploration

of the blocks and time spent with each block was determined. A rat was considered to be exploring a block when its head was oriented toward it and its nose was within a 2-cm radius.

Contextual and cued fear conditioning—Administration of the FC task includes 3 different phases, a training phase, a context test and a cue test and followed similar procedures as described previously (42). In all the 3 phases, rats were placed in a clear, acrylic chamber (30×30×40 cm^3 high; Pheno Typer 3000, Noldus Information Technology). On training and context test phases, the floor of the Pheno Typer contained a stainless steel grid. The fear-conditioning task began with a 15-minute training phase on day 1. Each rat was placed in the chamber, explored freely for 5 minutes to establish baseline-freezing behavior; next 5 minutes of training a series of 5 tone-shock pairings was administered. For each pairing, a 2,000 Hz, 90 dB tone was played for 30 seconds, and a mild (1 mA) footshock was administered concurrent with the final 1 second of the tone via the stainless steel grid floor. Following the final tone-shock pairing, rats were observed for an additional 5 minutes to assess posttraining freezing levels. The following day in the context test rats were allowed to freely explore for 5 minutes, and neither the tone nor shock stimuli were administered. If memory for the context-shock conditioned association is intact, rats will spend a significant proportion of the trial engaged in freezing behavior in response to being returned to the identical environment 24 hours later. The cue test phase was administered 1 hour after the context test phase was complete. For this phase, removing the stainless steel grid floor, adding panels to the sides of the fear conditioning chamber, and cleaning the floor of the chamber using a scented detergent solution all served to change the context. Rats explored freely for 5 minutes; for the first minute, no tone was played to assess pre-cue freezing in the altered context. During the following 3 minutes, the same tone was played as during training. Cue test freezing behavior was measured during this 3-minute period and for an additional minute after the tone was turned off.

BrdU injection and tissue processing—One week after irradiation, rats in all the groups received daily intraperitoneal injections of BrdU (5-bromo-2'-deoxyuridine, Sigma, St. Louis, MO) for 6 consecutive days at a dose of 100 mg/kg to assess addition of new stem/progenitor cells to the hippocampus. After 1 month to last BrdU injection rats were deeply anaesthetized with isofurane and perfused through the heart with 75 mL of phosphate buffered saline (PBS) containing heparin (10 U/mL, Sigma-Aldrich) followed by 350 mL of 4% paraformaldehyde in 0.1 M PBS (pH 7.4). The brains were removed, post-fixed in the same 4% paraformaldehyde solution for 24 hrs at 4 °C, cryoprotected using sucrose solution, and 30 μm-thick cryostat sections were cut coronally through the entire hippocampus and collected in PBS with 0.02% sodium azide.

Immunohistochemical assessment of radiation injury in the rodent brain—Immunohistochemical staining was undertaken to assess the scope of damage caused by the different irradiation modalities. Markers specific for newly born immature (doublecortin, DCX+) and mature (neuron specific nuclear antigen, NeuN+) neurons labeled with BrdU were used for the quantification of specific cell types between different regions of the irradiated brain. Additional markers of radiation injury were used to gauge the level of

inflammation by quantifying the activated microglia in different subfields of hippocampus (CD68 cell surface marker, ED1+).

Processing of tissue sections for immunostaining—To identify the expression of immature neurons, every 15th section through the entire hippocampus was selected in each animal and processed for DCX immunostaining. Sections were treated with 0.1 M PBS containing 20% methanol, 3% hydrogen peroxide, washed thoroughly in PBS, blocked in 10% normal horse serum, incubated overnight at 4 °C in DCX antibody (1:200, mouse monoclonal, Santa Cruz, CA). Avidin-biotin complex (ABC) method with Vector gray (Vector Labroratories, CA) as a chromogen was used to enhance the color development. Sections were mounted on Vectabond-coated slides (Vector Labs), air-dried, counterstained with nuclear fast red, dehydrated, cleared and cover slipped.

To identify mature neurons, representative sections were processed using dual immunofluorescence staining for BrdU and NeuN. Serial sections (every 15th) taken through entire hippocampus were selected. The free-floating sections were first rinsed in Tris-Buffered Saline (TBS, 0.1 M, pH 7.6) and subjected to BrdU pretreatment protocol using 50% formamide [made in 2× saline-sodium citrate (SSC) buffer; Sigma-Aldrich] at 69 °C for 2.5 hours and 2N HCl (Molcular Biology grade, Sigma-Aldrich, at 37 °C for 45 minutes), followed by serum blocking (10% normal donkey serum, NDS; Sigma-Aldrich) and overnight incubation in a BrdU antibody (1:200; rat monoclonal, AbD Serotec, NC). The sections were then treated with donkey anti-rat IgG Alexa Fluor 594 (1:200; Invitrogen, Life Technologies, CA) for 60 minutes, rinsed in PBS, blocked in serum, and incubated overnight with primary antibodies (mouse anti-NeuN, 1:500; Millipore, MA). The following day, sections were washed with PBS and treated with secondary antibody horse anti-mouse IgG Alexa Fluor 488 (1:200; Invitrogen, Life Technologies, CA). Immunostained sections were rinsed in PBS and mounted on clean Vectabond (Vector Labs) -treated slides using *SlowFade* anti-fade mounting medium (Invitrogen). BrdU+ cells (red) dual stained with NeuN (green) were visualized using laser scanning confocal microscopy.

To identify activated microglia (ED-1+ cells), sections were washed with PBS several times, blocked with 10% NDS in PBS containing 0.1% Triton X-100 for 30 minutes, and then incubated overnight in ED-1 antibody (monoclonal anti-rat CD68 raised in mouse, 1:500, AbD Serotec) prepared in PBS containing 2% NDS and 0.1% Triton X-100. On the second day, sections were washed and incubated for 1 hour in secondary antibody (donkey antimouse IgG Alexa Fluor 594, 1:200; Invitrogen). Sections were then washed thoroughly and counterstained with nuclear dye TOTO-3 iodide (1 μmol/L for 15 minutes; Invitrogen, Life Technologies) to visualize the different hippocampal cell layers.

Confocal analyses were carried out using multiple Z-stacks taken at 1 μm intervals using a confocal laser-scanning microscope (Nikon Eclipse TE2000-U, EZ-C1 interface, Nikon, Japan). Individual Z-sections were then analyzed using Nikon Elements software (version 3.2). The main determinant for the assessment of mature neurons in unilateral hippocampus irradiation was to determine percentage of BrdU-positive cells co-expressing mature neuronal marker, NeuN. At least 50 to 100 BrdU-positive cells were counted for each animal (6–8 serial sections). The percentage of dual-labeled BrdU-NeuN positive cells was

derived from 3 individual animals in each group. For quantifying the BrdU, every 15th section (30 μm thickness) through entire hippocampus (6–8 sections per animal) was included in the analysis, and positive cells were counted from 1-μm-thick Z-stacks scanned from 3 individual animals in each group. ED-1+ cells were quantified across hippocampal subfields (dentate hilus, DH; granule cell layer-subgranular zone, GCL-SGZ; and CA1 & 3 layers) and represented as the mean number of ED-1+ cells per hippocampal section. Data for DCX are represented as the mean number of DCX+ neurons in GCL-SGZ region per 30 μm section as quantified by bright field microscopy.

Statistical analyses

We used PASW Statistics 18 (SPSS, IBM Corporation, Somers, NY) for the statistical analyses of data. All statistical tests were 2-tailed, and a value of P≤;0.05 was considered statistically significant. In addition, normal distribution of the data (Kolmogorov-Smirnov test), and homogeneity of variance (Levene's test of equality of error variances) were confirmed for all the behavior data. When a statistically significant overall group effect was found, multiple comparisons were made using Fisher's protected least significant different (FPLSD) post hoc tests to compare the individual groups.

For the NPR task, exploration ratio, or the proportion of total time spent exploring the novel spatial location ($t_{novel}/t_{novel} + t_{familiar}$), was used as the main dependent measure. The behavior of the animals during minute 1 of the 5-minute test phase was analyzed.

For the FC task, percentage of time spent freezing was used as the main dependent measure. Freezing was assessed during the final minute of the 5-minute interval for baseline and post-training phases. For the context test, freezing was assessed over the entire 5-minute trial. For the pre-cue test, freezing was assessed during the first minute, in which no tone was sounded, and for the cue test, freezing was assessed across the three minute interval that the tone was sounded and for the final minute of the trial in which no tone was sounded. Repeated measures ANOVA was used to assess group (between subjects factor) and phase (within subjects factor) effects on freezing behavior [for details see ref. (42)].

Neurogenesis, proliferation and inflammation data (BrdU, DCX, BrdU-NeuN, ED1) are represented as Mean ± S.E.M. of 3–4 individual obervations. Data comparison was done using one-way ANOVA followed by Bonferroni's post hoc tests and a value of P≤0.05 was considered as statistically significant observation.

Results

Effects of targeted SRS on cognition

To gauge the functional consequences of our irradiation paradigms, NPR and FC cognitive testing was performed (Figure 5). One-way ANOVA revealed a significant overall group effect on the NPR task (P<0.0001). Post hoc tests show that whole-brain IRR animals (wbIRR) spent a significantly decreased proportion of time exploring the novel spatial position compared to all other groups (P's<0.004). The control, uhIRR and hIRR groups did not differ, however only control (P=0.002) and hIRR (P=0.002) animals spent significantly more time exploring the novel place than expected by chance (Figure 5A). For the FC task,

repeated measures ANOVA revealed a significant group X phase interaction (P=0.007). Individual ANOVAs conducted for each phase of the task reveal significant group differences on both the post-training phase (P=0.002) and the context test (P=0.003, Figure 5B). Post hoc tests for the post-training phase show that hIRR animals spent less time freezing than all other groups (*P's<0.03). For the hippocampal-dependent context phase, hIRR and wbIRR animals spent less time freezing than controls (#P's<0.006), uhIRR animals did not differ from controls (Figure 5B). Also, uhIRR animals differed significantly from hIRR animals (P=0.011) and showed a trend to spend more time freezing than wbIRR animals (P=0.09).

Immunohistochemical assessment of unilaterally irradiated brains: doublecortin (DCX) staining of immature neurons

To corroborate the success of our treatment plan to target the contoured brain region of interest, immunohistochemical staining for radiation injury was undertaken. SRS (10 Gy) targeted to a single hippocampus showed that the number of DCX+ immature neurons was reduced significantly by 80% on the ipsilateral side (Figure 6B,D) and elevated by 22% on the contralateral side (Figure 6C,D) when compared to non-irradiated animals (control, 51±3.0; ipsilateral, 10±1.0; contralateral, 62±4.92; control *vs*. ipsilateral, P<0.001). DCX-positive neurons extended their dendrites into the inner molecular layer of the dentate gyrus, particularly evident in control animals (Figure 6A). Furthermore qualitative observation showed that the reduced number of DCX+ neurons in the ipsilateral hippocampus are less complex compared to neurons subjected to lower total doses. Thus, SRS reduced the number of DCX+ cells to a far greater extent on the targeted (ipsilateral) side, compared to that found on the non-targeted (contralateral) side receiving a mean dose of 1.5 Gy (Figure 3).

Immunohistochemical assessment of unilaterally irradiated brains: NeuN staining of mature neurons

Further examination of unilateral irradiated brains showed that the number of mature (NeuN +) neurons co-labeled with BrdU following irradiation were also significantly reduced (Figure 7) on the ipsilateral side. Analysis of the GCL-SGZ region of the unilaterally irradiated hippocampus revealed that the percentage of cells co-labeled with BrdU that express NeuN on the ipsilateral side was 48%, while on the contralateral side was 90% at 6 weeks after irradiation (control, 56±2.6; ipsilateral, 48±4.3; contralateral, 90±1.8; control *vs*. ipsilateral, P<0.05; ipsilateral *vs*. contralateral, P<0.001; Figure 7). The reduced percentage of BrdU+ cells expressing NeuN on the ipsilateral versus contralateral sides of the unilaterally irradiated brain further confirm our capability to accurately and differentially irradiate the rodent brain.

Immunohistochemical assessment of unilaterally irradiated brains: ED1 staining of activated microglia

To determine how partial irradiation of the brain might impact neuroinflammation, an assessment of activated microglia using ED1 immunostaining was undertaken. Unilateral irradiation of the hippocampus induced a chronic inflammation on both ipsilateral and contralateral sides of the hippocampus as quantified by the number of activated microglia

immunoreactive for ED1 (Figure 8). However, the number of activated microglia (ED1+) was found to be significantly higher on the ipsilateral versus contralateral sides (Figure 8). Quantifying the yields of activated microglia throughout different subfields of the hippocampus revealed that the CA1 and CA3 regions showed the highest levels of ED1+ cells compared to the DH and GCL (Figure 8). For the ipsilateral hippocampus, the yields of ED1+ cells in the DH (control, 6.2±0.38; ipsilateral, 20.5±0.25; $P<0.001$), GCL (control, 8.0±0.44; ipsilateral, 24±2.1; $P<0.01$), and the CA1 and CA3 (control, 5.2±0.88; ipsilateral, 46±1.3; $P<0.001$) were analyzed 6 weeks after irradiation as compared to unirradiated controls (Figure 8) For the contralateral hippocampus, the yields of ED1+ cells in the DH, GCL and CA1/CA3 subfields were 9.0±0.50 ($P<0.05$), 9.0±0.88 and 16±0.40 ($P<0.01$) respectively, when compared to unirradiated controls (Figure 8). These data clearly indicate a persistent level of inflammation in the unilaterally irradiated brain, where the yield of ED1+ cells in all subfields of the ipsilateral hippocampus exceeds those levels found on the contralateral side.

Discussion

The capability to more accurately target radiation to defined volumes of the brain facilitates the killing of cancer cells while sparing normal tissue adjacent and distal to the disease site. Improved beam delivery technologies have stimulated the widespread use of various forms of SRS to deliver larger doses to the tumor bed while minimizing normal tissue damage (43,44). This is particularly important for the brain, since neurodegenerative sequelae are common in patients subjected to cranial irradiation for the treatment of a variety of CNS malignancies (45,46). Past work from us has defined the adverse effects of irradiation on cognition, where rodents subjected to an acute, head only dose of 10 Gy showed performance decrements on the NPR task 1 and 4 months following irradiation (37,38,47). In the present study, we have expanded our past work to further define the types of cognitive decrements resulting from the targeted irradiation of one or both hippocampi, with follow up immunohistochemical analyses to determine the cellular consequences of such exposures.

Animals subjected to SRS under the stated conditions exhibited performance decrements when assessed by NPR and FC behavioral tasks (Figure 5). Similar to past findings (47) whole brain irradiation (wbIRR) led to significantly reduced exploration ratios when compared to unirradiated controls (Figure 5A). Reduced tendencies to explore novelty were not found following SRS targeted to one (uhIRR) or both hippocampi (hIRR) and this suggests that sparing the whole brain may help preserve cognitive function (Figure 5A). Cognitive decrements were more pronounced when animals were assessed on the FC task. A decrement in post-training learning was found in animals subjected to SRS targeting both hippocampi (Figure 5B), an effect not found in the other experimental cohorts. However, an assessment of animals on the hippocampal-dependent context version of the FC task revealed significant decrement in animals receiving SRS targeted to both hippocampi or the whole brain (Figure 5B). Interestingly, targeting a single hippocampus did not lead to deficits on the context version of this cognitive test. None of the experimental cohorts showed significant deficits in the cued version of the FC task, known to interrogate the amygdala to a greater extent. Collectively, cognitive data derived from 2 sensitive hippocampal tasks point to significant deficits following wbIRR, while SRS targeted to one

or both hippocampi resulted in less severe decrement depending on the particular task. Data also indicated that irradiation of both hippocampi was more deleterious than irradiating one hippocampus (Figure 5B) suggesting a possible compensatory response within the irradiated brain.

To explore the possibility that differential responses to localized injury in the hippocampus might serve to compensate for radiation-induced functional changes we analyzed the ispsilateral and contralateral hemispheres for changes in neurogenesis and inflammation. The reduction of radiosensitive populations of neural stem and precursor cells in the neurogeneic regions of the brain have long been associated with the inhibition of neurogenesis and the onset of hippocampus-dependent deficits in learning and memory (18,19). Recent work has used image-guided radiotherapy to define the dose-response relationships for the neurogenic cells in the rat hippocampus (48). Data showed that dose-dependent reductions in neurogenesis could be partially offset by proliferation at lower doses but not at doses exceeding 5 Gy (48). In the current study, we sought to expand past work from us and others by analyzing the consequences of SRS on cognition and linking such functional changes to regional differences in the radioresponse of the different hippocampal subfields. Present data demonstrating significant reductions in DCX+ and BrdU+/NeuN+ cells in the ipsilateral hemisphere of the brain following SRS, validates our capability to target individual hippocampi using our treatment plan. A mean dose of 10 Gy to the ipsilateral hippocampus led to significant reductions in the number of immature (80%, DCX+) and mature neurons (27%, BrdU+/NeuN+) (Figures 6,7). The lower mean dose (1.5 Gy) to the contralateral hippocampus was however, found to increase the yield of these same newly born neurons significantly, where DCX+ and BrdU+/NeuN+ cells increased by 22% and 36% respectively (Figures 6,7). Thus, while the irradiated hemisphere showed marked reductions in neurogenesis, the unirradiated hemisphere did not. The unexpected high levels of neurogenesis on the contralateral side of the brain suggest, that compensatory mechanisms may operate in response to distal radiation injury to increase the functional (cognitive) reserve of the CNS. Our data demonstrate for the first time differential responses of the partially irradiated brain, and the capability of the CNS to respond to radiation injury to increase proliferation of neurogenic stem cell compartments receiving lower total doses than regions directly targeted by SRS treatment plans.

To explore additional factors that might impact the differential neurogenic responses within the unilaterally irradiated brain, activated microglia were quantified as a marker for neuroinflammation. The yield of activated microglia was elevated significantly in the ipsilateral hemisphere, with more modest increases found in the contralateral hemisphere compared to controls (Figure 8). These results track expected dose-dependent responses, where elevations in neuroinflammation may act to inhibit neurogenesis on the ipsilateral side, but due to the relatively lower yields of activated microglia on the contralateral side, inflammatory signaling may be insufficient to exert inhibitory effects on neurogenesis. Past work has found that microglia are detrimental to the neurogenic process (49) and in a chemokine (C-C motif) receptor-2 (CCR2) deficient animal model that impairs microgial activation, radiation-induced cognitive decrements were prevented (50). In a transgenic mouse model of Alzheimer's disease, inhibition of microglial activation was found to be beneficial for neurogenesis and cognition (51). Neuroinflammation has many diverse effects

in the brain and influences the functional integration of newly born neurons, possibly through the activation of microglia (52,53). While the issue of whether microglia are beneficial or deleterious in various injury models of the brain remains unresolved (53,54), our data point to the importance of microglia in the process of neurogenesis following irradiation.

Collectively our data demonstrate that hippocampal-targeted unilateral irradiation of the brain elicits performance decrements on hippocampal-dependent behavioral tasks. Cognitive deficits are coincident with significant radiation-induced reductions in neurogenesis and enhanced inflammation in the ipsilateral hemisphere. Interestingly, on the contralateral hemisphere receiving a lower total dose, neurogenesis was increased while the relative level of activated microglia was significantly lower when compared to the opposing hemisphere. These results suggest that the response to radiation injury is dynamic and complex, with the capability to compensate for distant injury that is likely dose-dependent.

Acknowledgments

This work was supported by the National Institutes of Health NINDS Grant R01 NS074388 (CLL).

References

1. Fike JR, Rosi S, Limoli CL. Neural precursor cells and central nervous system radiation sensitivity. Semin Radiat Oncol. 2009; 19:122–132. [PubMed: 19249650]
2. Barani IJ, Benedict SH, Lin PS. Neural stem cells: implications for the conventional radiotherapy of central nervous system malignancies. Int J Radiat Oncol Biol Phys. 2007; 68:324–333. [PubMed: 17398036]
3. Gutiérrez AN, Westerly DC, Tomé WA, et al. Whole brain radiotherapy with hippocampal avoidance and simultaneously integrated brain metastases boost: a planning study. Int J Radiat Oncol Biol Phys. 2007; 69:589–597. [PubMed: 17869672]
4. Marsh JC, Godbole RH, Herskovic AM, et al. Sparing of the neural stem cell compartment during whole-brain radiation therapy: a dosimetric study using helical tomotherapy. Int J Radiat Oncol Biol Phys. 2010; 78:946–954. [PubMed: 20472348]
5. Gerosa M, Nicolato A, Foroni R. The role of gamma knife radiosurgery in the treatment of primary and metastatic brain tumors. Curr Opin Oncol. 2003; 15:188–196. [PubMed: 12778010]
6. Kollová A, Liscák R, Novotný J Jr, et al. Gamma Knife surgery for benign meningioma. J Neurosurg. 2007; 107:325–336. [PubMed: 17695387]
7. Swennen MH, Bromberg JE, Witkamp TD, et al. Delayed radiation toxicity after focal or whole brain radiotherapy for low-grade glioma. J Neurooncol. 2004; 66:333–339. [PubMed: 15015665]
8. Crossen JR, Garwood D, Glatstein E, et al. Neurobehavioral sequelae of cranial irradiation in adults: a review of radiation-induced encephalopathy. J Clin Oncol. 1994; 12:627–642. [PubMed: 8120563]
9. Abayomi OK. Pathogenesis of irradiation-induced cognitive dysfunction. Acta Oncol. 1996; 35:659–663. [PubMed: 8938210]
10. Meyers CA. Neurocognitive dysfunction in cancer patients. Oncology (Williston Park). 2000; 14:75–79. discussion 79, 81–2, 85. [PubMed: 10680150]
11. Anderson VA, Godber T, Smibert E, et al. Cognitive and academic outcome following cranial irradiation and chemotherapy in children: a longitudinal study. Br J Cancer. 2000; 82:255–262. [PubMed: 10646874]
12. Meyers CA, Brown PD. Role and relevance of neurocognitive assessment in clinical trials of patients with CNS tumors. J Clin Oncol. 2006; 24:1305–1309. [PubMed: 16525186]

13. Fike JR, Rola R, Limoli CL. Radiation response of neural precursor cells. Neurosurg Clin N Am. 2007; 18:115–127. x. [PubMed: 17244559]
14. Tofilon PJ, Fike JR. The radioresponse of the central nervous system: a dynamic process. Radiat Res. 2000; 153:357–370. [PubMed: 10798963]
15. Kim JS, Lee HJ, Kim JC, et al. Transient impairment of hippocampus-dependent learning and memory in relatively low-dose of acute radiation syndrome is associated with inhibition of hippocampal neurogenesis. J Radiat Res. 2008; 49:517–526. [PubMed: 18574327]
16. Mizumatsu S, Monje ML, Morhardt DR, et al. Extreme sensitivity of adult neurogenesis to low doses of X-irradiation. Cancer Res. 2003; 63:4021–4027. [PubMed: 12874001]
17. Monje ML, Mizumatsu S, Fike JR, et al. Irradiation induces neural precursor-cell dysfunction. Nat Med. 2002; 8:955–962. [PubMed: 12161748]
18. Raber J, Rola R, LeFevour A, et al. Radiation-induced cognitive impairments are associated with changes in indicators of hippocampal neurogenesis. Radiat Res. 2004; 162:39–47. [PubMed: 15222778]
19. Rola R, Raber J, Rizk A, et al. Radiation-induced impairment of hippocampal neurogenesis is associated with cognitive deficits in young mice. Exp Neurol. 2004; 188:316–330. [PubMed: 15246832]
20. Zhao C, Deng W, Gage FH. Mechanisms and functional implications of adult neurogenesis. Cell. 2008; 132:645–660. [PubMed: 18295581]
21. Fishman K, Baure J, Zou Y, et al. Radiation-induced reductions in neurogenesis are ameliorated in mice deficient in CuZnSOD or MnSOD. Free Radic Biol Med. 2009; 47:1459–1467. [PubMed: 19703553]
22. Rola R, Zou Y, Huang TT, et al. Lack of extracellular superoxide dismutase (EC-SOD) in the microenvironment impacts radiation-induced changes in neurogenesis. Free Radic Biol Med. 2007; 42:1133–1145. discussion 1131–2. [PubMed: 17382195]
23. Monje ML, Toda H, Palmer TD. Inflammatory blockade restores adult hippocampal neurogenesis. Science. 2003; 302:1760–1765. [PubMed: 14615545]
24. Andres-Mach M, Rola R, Fike JR. Radiation effects on neural precursor cells in the dentate gyrus. Cell Tissue Res. 2008; 331:251–262. [PubMed: 17786480]
25. Tada E, Parent JM, Lowenstein DH, et al. X-irradiation causes a prolonged reduction in cell proliferation in the dentate gyrus of adult rats. Neuroscience. 2000; 99:33–41. [PubMed: 10924950]
26. Brown WR, Blair RM, Moody DM, et al. Capillary loss precedes the cognitive impairment induced by fractionated whole-brain irradiation: a potential rat model of vascular dementia. J Neurol Sci. 2007; 257:67–71. [PubMed: 17316691]
27. Lamproglou I, Baillet F, Boisserie G, et al. The influence of age on radiation-induced cognitive deficit:experimental studies on brain irradiation of 30 gy in 10 sessions and 12 hours in the Wistar rat at 1 1/2, 4 and 18 months age. Can J Physiol Pharmacol. 2002; 80:679–685. [PubMed: 12184320]
28. Madsen TM, Kristjansen PE, Bolwig TG, et al. Arrested neuronal proliferation and impaired hippocampal function following fractionated brain irradiation in the adult rat. Neuroscience. 2003; 119:635–642. [PubMed: 12809684]
29. Shi L, Linville MC, Iversen E, et al. Maintenance of white matter integrity in a rat model of radiation-induced cognitive impairment. J Neurol Sci. 2009; 285:178–184. [PubMed: 19625028]
30. Zhao W, Payne V, Tommasi E, et al. Administration of the peroxisomal proliferator-activated receptor gamma agonist pioglitazone during fractionated brain irradiation prevents radiation-induced cognitive impairment. Int J Radiat Oncol Biol Phys. 2007; 67:6–9. [PubMed: 17189061]
31. Duan XQ, Wu HX, Liu HL, et al. Expression and changes of Fos protein in the rat forebrain after gamma knife irradiation targeted to the caudate putamen. Neurosurgery. 1999; 45:139–145. discussion 145–6. [PubMed: 10414576]
32. Duan XQ, Wu SL, Li T, et al. Expression and significance of three types of Fos-immunoreactive cells after gamma knife irradiation of the forebrain in the rat. Neurosci Res. 1999; 33:99–104. [PubMed: 10211774]

33. Hirano M, Rakwal R, Kouyama N, et al. Gel-based proteomics of unilateral irradiated striatum after gamma knife surgery. J Proteome Res. 2007; 6:2656–2668. [PubMed: 17564426]
34. Hirano M, Shibato J, Rakwal R, et al. Transcriptomic analysis of rat brain tissue following gamma knife surgery: early and distinct bilateral effects in the un-irradiated striatum. Mol Cells. 2009; 27:263–268. [PubMed: 19277511]
35. Rao ZR, Ge X, Qiou JY, et al. Expression and changes of HSP70 in the rat forebrain subjected to gamma knife (100Gy) irradiation targeted on the caudate putamen and survived for different times. Neurosci Res. 2000; 38:139–146. [PubMed: 11000440]
36. Yang T, Wu SL, Liang JC, et al. Time-dependent astroglial changes after gamma knife radiosurgery in the rat forebrain. Neurosurgery. 2000; 47:407–415. discussion 415–6. [PubMed: 10942014]
37. Acharya MM, Christie LA, Lan ML, et al. Rescue of radiation-induced cognitive impairment through cranial transplantation of human embryonic stem cells. Proc Natl Acad Sci U S A. 2009; 106:19150–19155. [PubMed: 19901336]
38. Acharya MM, Christie LA, Lan ML, et al. Human neural stem cell transplantation ameliorates radiation-induced cognitive dysfunction. Cancer Res. 2011; 71:4834–4845. [PubMed: 21757460]
39. Leksell L. The stereotaxic method and radiosurgery of the brain. Acta Chir Scand. 1951; 102:316–319. [PubMed: 14914373]
40. Roa DE, Schiffner DC, Zhang J, et al. The use of RapidArc volumetric-modulated arc therapy to deliver stereotactic radiosurgery and stereotactic body radiotherapy to intracranial and extracranial targets. Med Dosim. 2012; 37:257–264. [PubMed: 22365418]
41. Almond PR, Biggs PJ, Coursey BM, et al. AAPM's TG-51 protocol for clinical reference dosimetry of high-energy photon and electron beams. Med Phys. 1999; 26:1847–1870. [PubMed: 10505874]
42. Christie LA, Acharya MM, Parihar VK, et al. Impaired cognitive function and hippocampal neurogenesis following cancer chemotherapy. Clin Cancer Res. 2012; 18:1954–1965. [PubMed: 22338017]
43. Barani IJ, Cuttino LW, Benedict SH, et al. Neural stem cell-preserving external-beam radiotherapy of central nervous system malignancies. Int J Radiat Oncol Biol Phys. 2007; 68:978–985. [PubMed: 17467925]
44. Blomstrand M, Brodin NP, Munck Af, Rosenschöld P, et al. Estimated clinical benefit of protecting neurogenesis in the developing brain during radiation therapy for pediatric medulloblastoma. Neuro Oncol. 2012; 14:882–889. [PubMed: 22611031]
45. Abayomi OK. Pathogenesis of cognitive decline following therapeutic irradiation for head and neck tumors. Acta Oncol. 2002; 41:346–351. [PubMed: 12234025]
46. Butler JM, Rapp SR, Shaw EG. Managing the cognitive effects of brain tumor radiation therapy. Curr Treat Options Oncol. 2006; 7:517–523. [PubMed: 17032563]
47. Acharya MM, Christie LA, Lan ML, et al. Comparing the functional consequences of human stem cell transplantation in the irradiated rat brain. Cell Transplant. 2013; 22:55–64. [PubMed: 22546529]
48. Tan YF, Rosenzweig S, Jaffray D, et al. Depletion of new neurons by image guided irradiation. Front Neurosci. 2011; 5:59. [PubMed: 21541259]
49. Ekdahl CT, Claasen JH, Bonde S, et al. Inflammation is detrimental for neurogenesis in adult brain. Proc Natl Acad Sci U S A. 2003; 100:13632–13637. [PubMed: 14581618]
50. Belarbi K, Jopson T, Arellano C, et al. CCR2 deficiency prevents neuronal dysfunction and cognitive impairments induced by cranial irradiation. Cancer Res. 2013; 73:1201–1210. [PubMed: 23243025]
51. Biscaro B, Lindvall O, Tesco G, et al. Inhibition of microglial activation protects hippocampal neurogenesis and improves cognitive deficits in a transgenic mouse model for Alzheimer's disease. Neurodegener Dis. 2012; 9:187–198. [PubMed: 22584394]
52. Jakubs K, Bonde S, Iosif RE, et al. Inflammation regulates functional integration of neurons born in adult brain. J Neurosci. 2008; 28:12477–12488. [PubMed: 19020040]
53. Ekdahl CT. Microglial activation - tuning and pruning adult neurogenesis. Front Pharmacol. 2012; 3:41. [PubMed: 22408626]

54. Ekdahl CT, Kokaia Z, Lindvall O. Brain inflammation and adult neurogenesis: the dual role of microglia. Neuroscience. 2009; 158:1021–1029. [PubMed: 18662748]

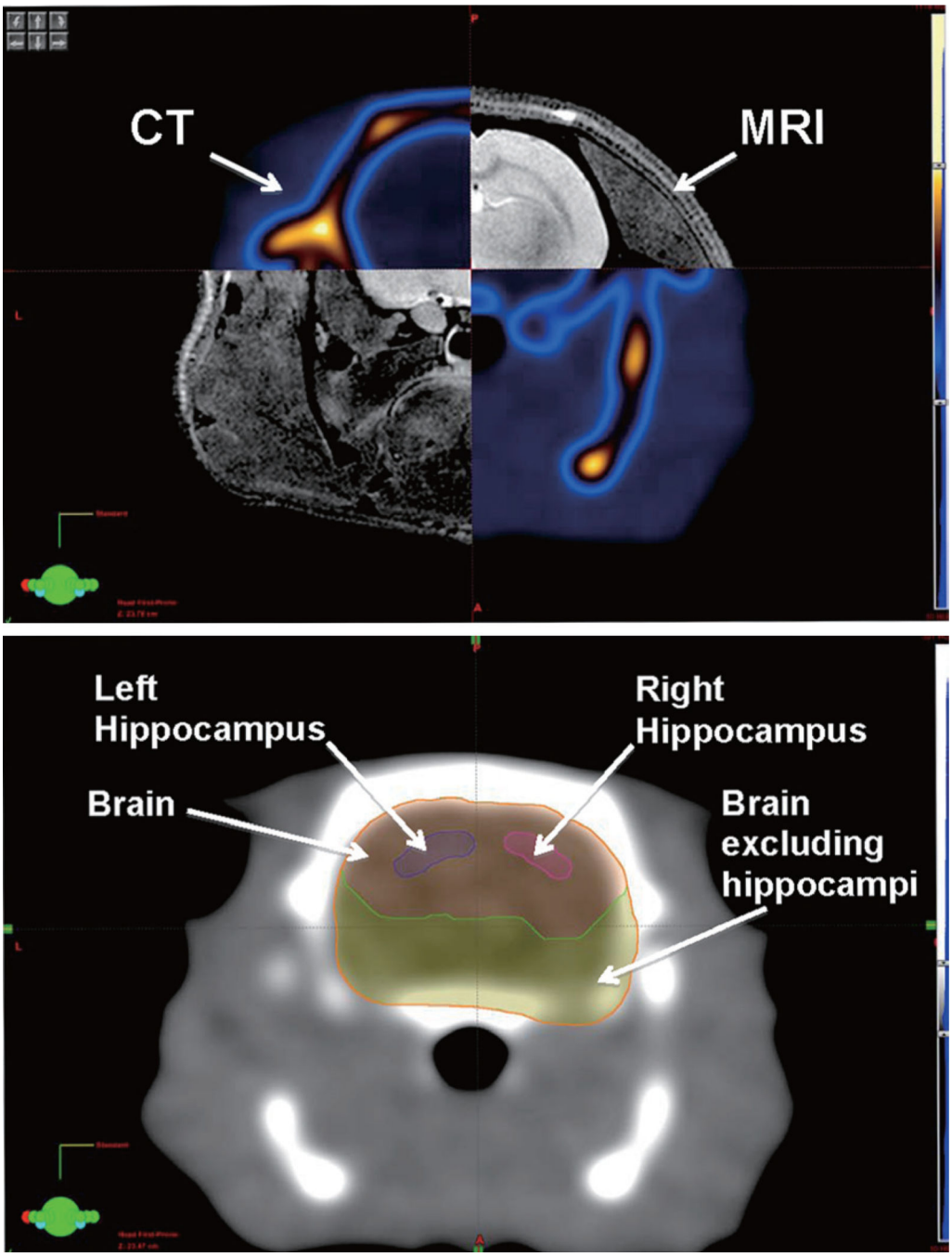

Figure 1.

Axial CT and MRI studies of the ATN rat brain fused in Eclipse treatment planning software (top). Contours of the left and right hippocampus, brain and brain excluding the hippocampi are shown (bottom). All the contours were created in Eclipse (bottom)

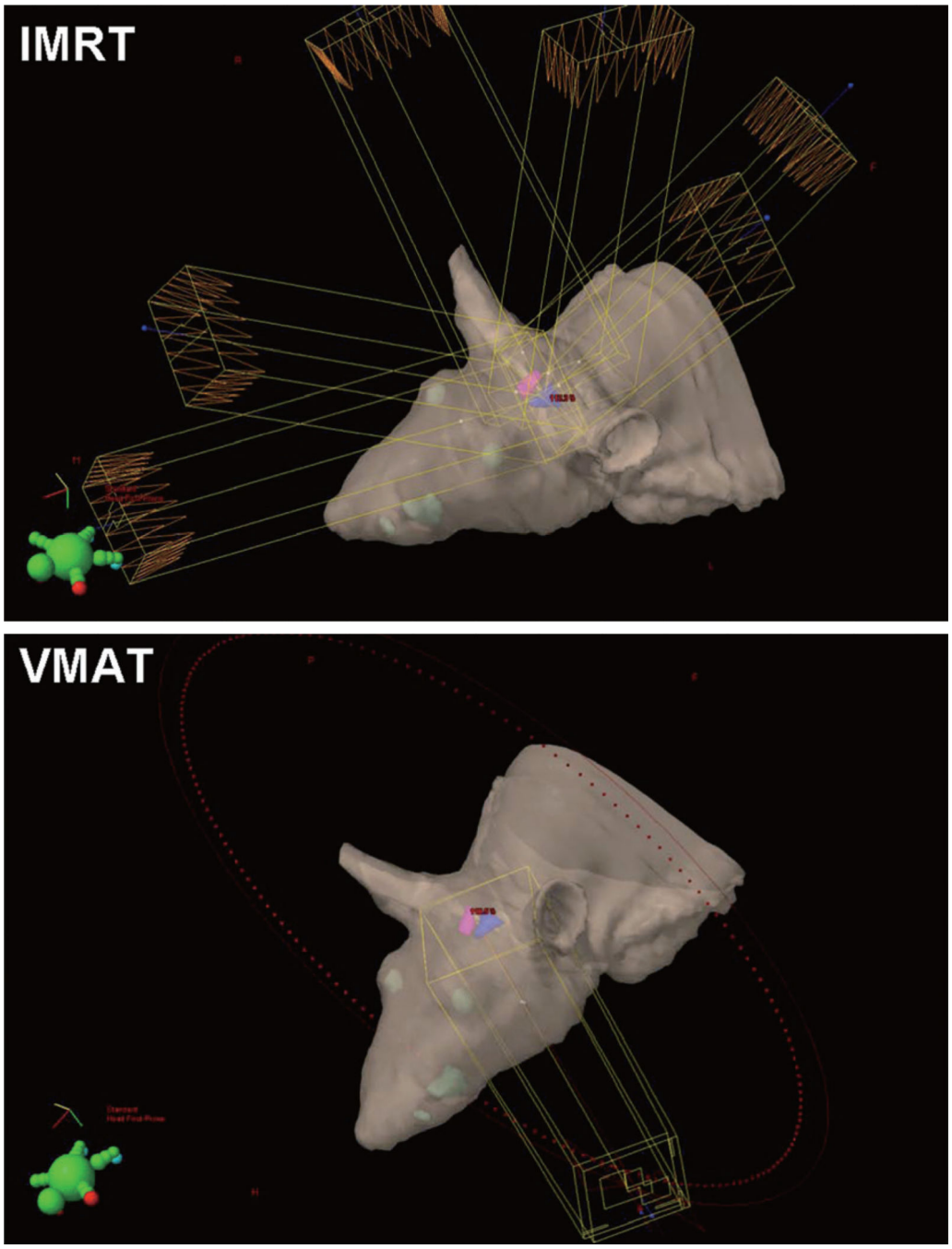

Figure 2.
Three-dimensional rendering of an ATN rat depicting the non-coplanar 6-field IMRT treatment technique used for a single hippocampus irradiation (top) and the 2 axial 358° arcs used VMAT treatment for both hippocampi (bottom)

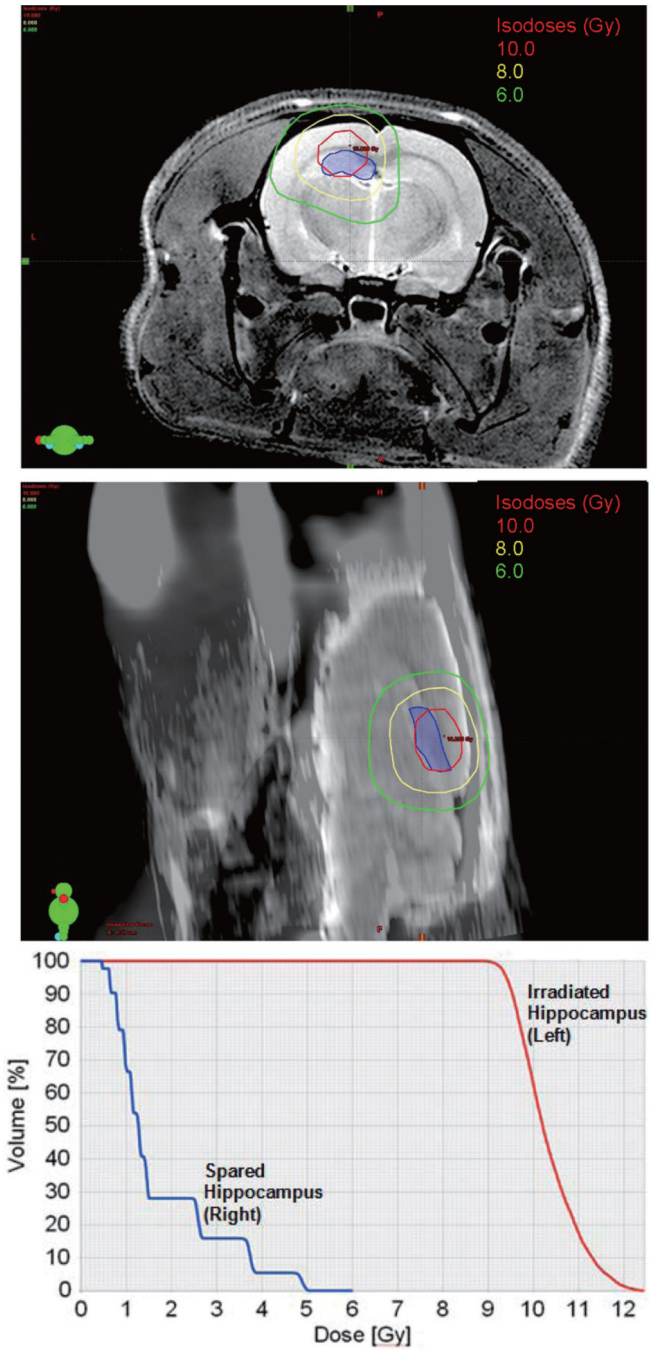

Figure 3.

Dose distribution showing the 10, 8 and 6 Gy isodose lines calculated in Eclipse for the single hippocampus irradiation and shown in the axial view (top). The same dose distribution but shown in the sagittal view (middle). Dose volume histogram for the irradiated (red) and the non-irradiated (blue) hippocampi. The irradiated hippocampus received a dose of 10 Gy in one single fraction. The dose sparing achieved was remarkable due to the close proximity (≤2 mm) of the hippocampus (bottom)

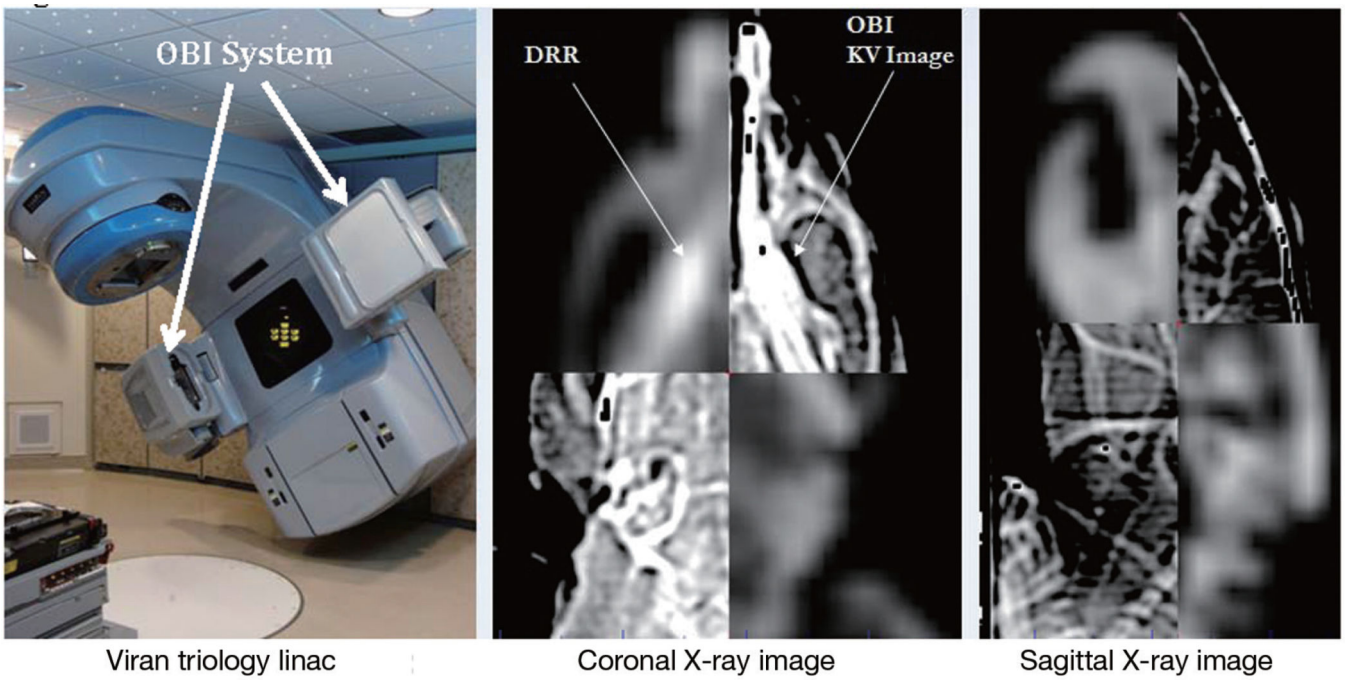

Figure 4.

Photograph of the Varian Trilogy linear accelerator (LINAC) used for the irradiation and with the OBI (on-board imaging) system indicated (left). Coronal view of the co-registration of the digitally reconstructed radiographs (DRRs) and the diagnostic quality X-ray image acquired with the OBI system (middle). Sagittal view of the co-registration is shown

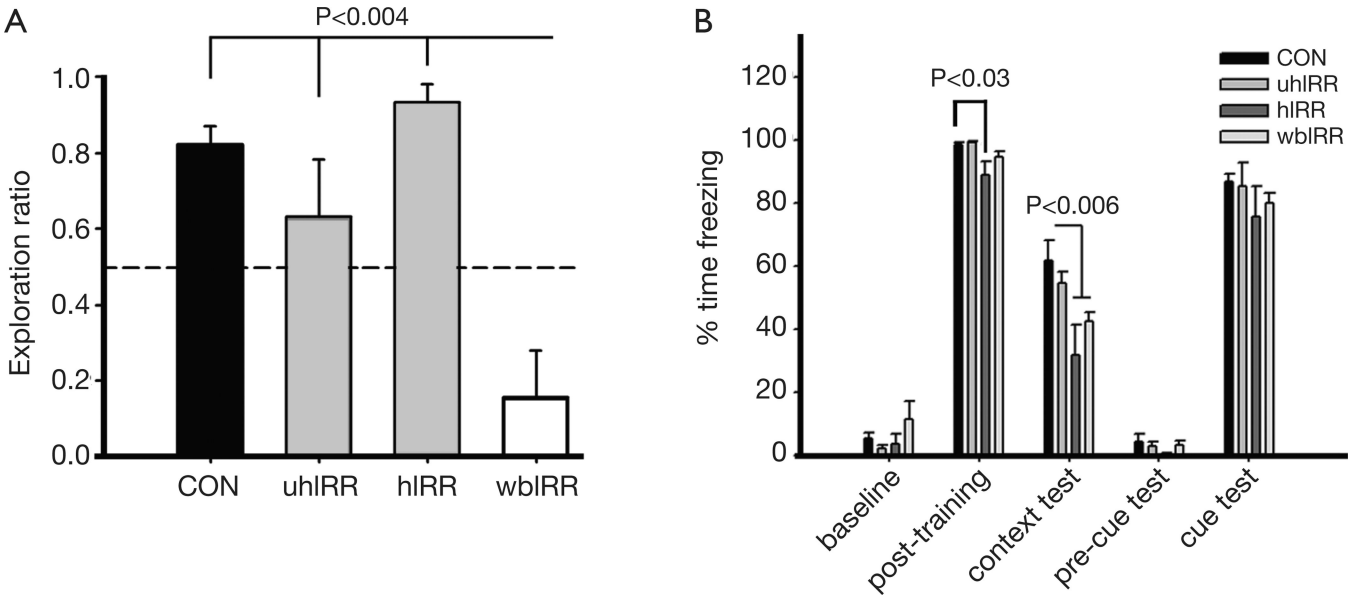

Figure 5.

Whole-brain, but not unilateral or bilateral hippocampus, irradiation impairs recognition memory as assessed by a novel place recognition task (A). During the 5-minute test, wbIRR spent a significantly reduced proportion of time exploring the novel place compared to CON, animals receiving unilateral (uhIRR) or bilateral hippocampal-10 Gy irradiation (hIRR). The exploration ratios of animals receiving unilateral or bilateral hippocampal 10 Gy irradiation (hIRR) did not differ significantly from controls. In contrast, bilateral hippocampal (hIRR) and whole-brain irradiation (wbIRR) impair hippocampal-dependent contextual fear conditioning memory (B). Unilateral hippocampal (uhIRR), hIRR and wbIRR groups did not differ from controls in the proportion of time spent freezing during initial exposure to the apparatus (baseline) nor following a series of 5 tone-shock pairings (post-training). When returned to the same context 24hr later, however, both hIRR and wbIRR groups spent significantly less time freezing compared to control, indicating impaired memory for the context in which they had received the tone-shock pairings. By contrast, when exposed to a new context 1hr later (pre-cue) and following sounding of the tone in this new context (cue test), hIRR and wbIRR animals were not impaired. Data shown are means +1 SEM, and the dashed lines in (A) represent chance performance (i.e., 0.5)

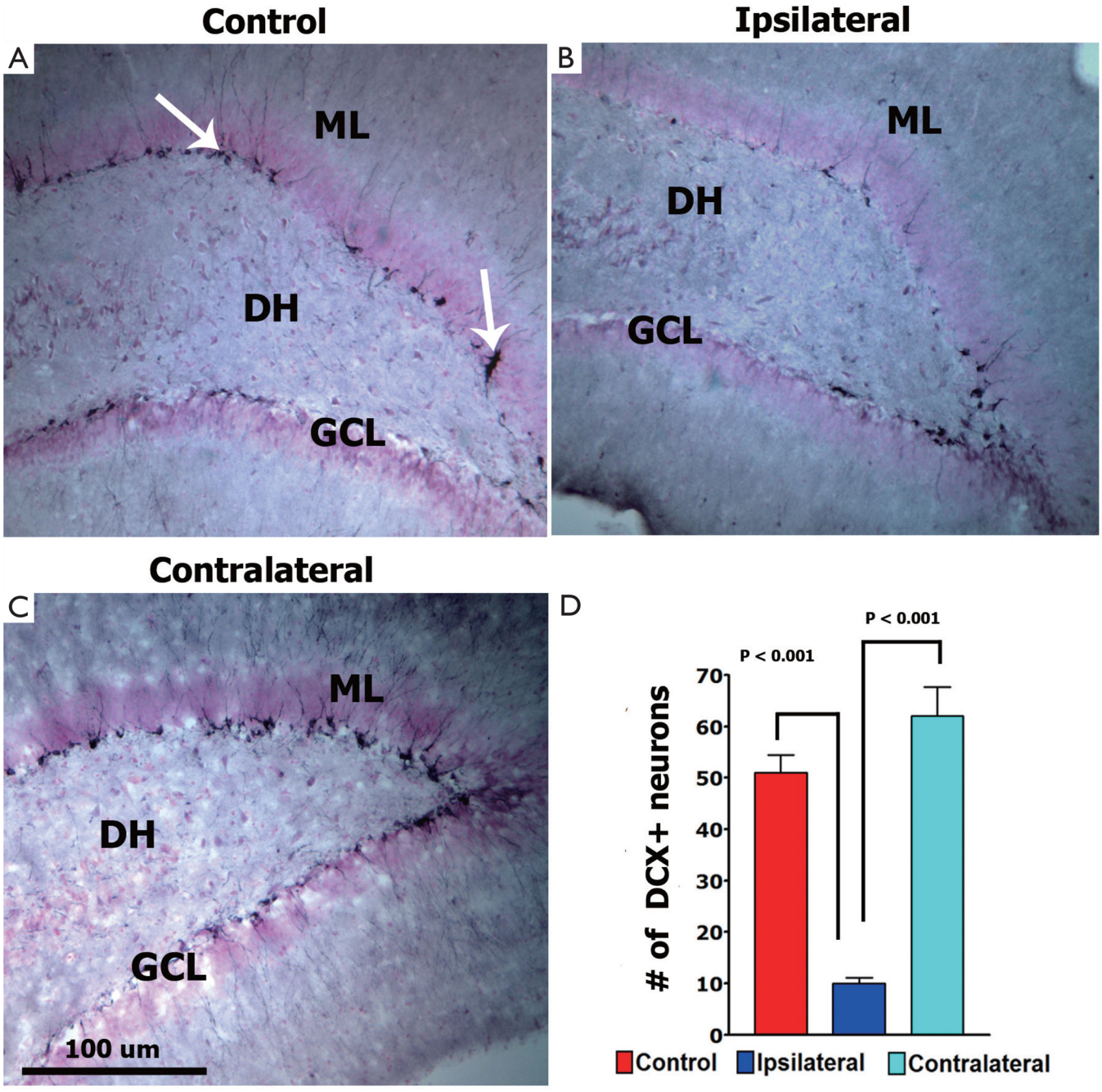

Figure 6.

Digital photomicrographs of early neurogenesis in the dentate gyrus as analyzed by DCX immunostaining (A–C). The ipsilateral hippocampus (B) showed reduced (80%, P<0.001) numbers of DCX-positive newly born neurons while the contralateral hippocampus showed increased (20%) numbers of these cells compared to unirradiated controls. Bar chart (D) shows the quantification of DCX-positive cells (arrows) in the unilaterally irradiated (10 Gy) brain

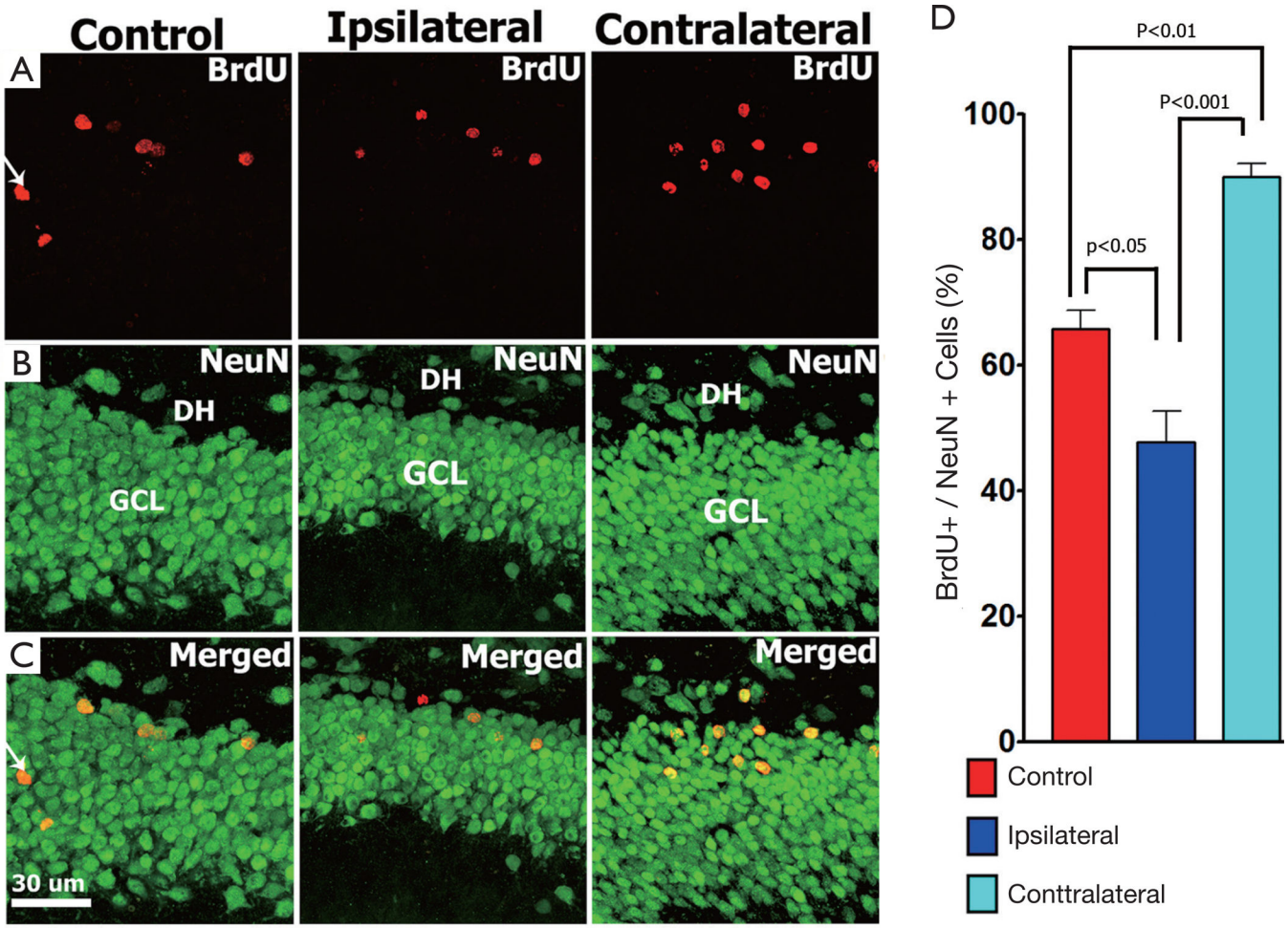

Figure 7.

Neurogenesis in the unilaterally irradiated brain. Images from the SGZ-GCL region of the hippocampus shows BrdU-positive (A-panels red), NeuN-positive (B-panels, green) and the cells that are co-labeled (C-panels). Targeted SRS reduced significantly the percentage of BrdU positive cells that express NeuN in the ipsilateral hippocampus (C). The majority of BrdU-positive cells expressing NeuN were found in the contralateral SGZ-GCL (C) at 6-weeks postirradiation. Bar chart (D) shows the percentage of BrdU-positive cells co-labeled with NeuN in the ipsilateral (43%) and contralateral (90%) hemispheres compared to non-irradiated controls (64%)

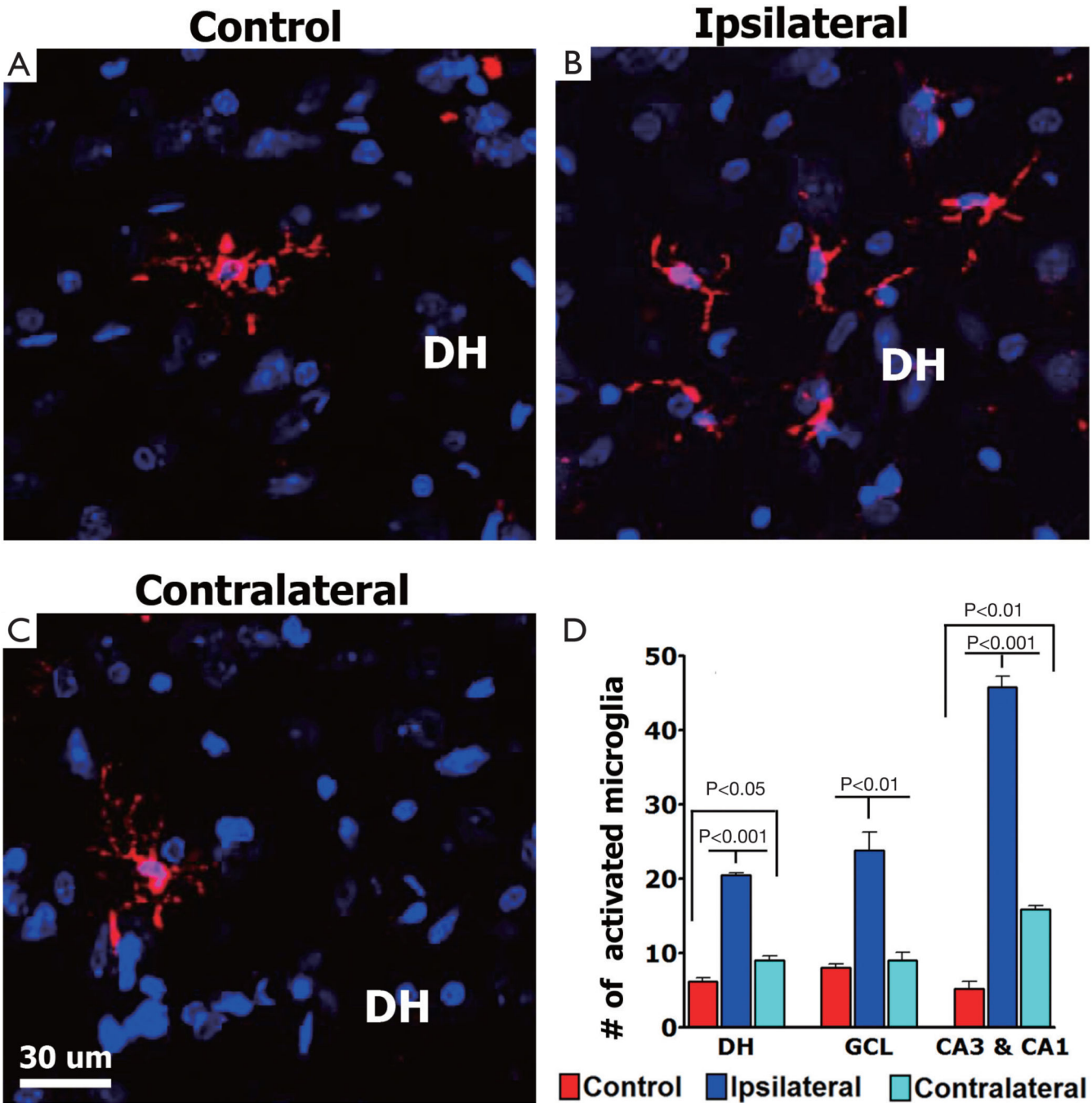

Figure 8.

Neuroinflammation in the unilaterally irradiated brain. Immunohistochemical staining for ED1-positive activated microglia in different subfields of the hippocampus 6 weeks after irradiation. (A) Control, (B) ipsilateral, (C) contralateral and (D) bar chart shows the number of activated microglia in each group. Quantification of activated microglia showed chronic inflammation throughout the hippocampus, with the highest levels in the ipsilateral versus contralateral hemispheres. Significant changes for the ipsilateral hippocampus (DH,

P<0.001; GCL, P<0.01; CA1/CA3, P<0.001) and the contralateral hippocampus (DH, P<0.05: CA1/CA3, P<0.001) are indicated as compared to non-irradiated controls